

S-BAND PHOTOINJECTOR INVESTIGATIONS BY MULTI-OBJECTIVE GENETIC OPTIMIZER*

H. Qian[#], D. Filippetto, F. Sannibale, LBNL, Berkeley, CA 94720, USA

Abstract

Photoinjectors has witnessed great progress in the past few decades, with low duty cycle high gradient guns, such as normal conducting S/L band gun, pushing the peak beam brightness frontier, and CW guns, such as DC gun, SRF gun and VHF gun, pushing the average beam brightness frontier. Due to different degrees of complexity, pulsed high gradient photoinjectors are usually optimized by manual scans, while CW photoinjectors are optimized by multi-objective genetic optimizers. In this paper, a multi-objective genetic optimizer is used to revisit S-band photoinjector beam brightness optimizations, showing a trade-off between peak current and transverse emittance, with the optimized injector layout depending on bunch charge and peak current. For 200 pC case, the final beam core brightness at injector exit is close to cathode maximum brightness in the ‘cigar beam’ regime. Assuming a thermal emittance of 0.5 $\mu\text{m}/\text{mm}$ and a beam charge of 200 pC, about 90 nm slice emittance at 20 A peak current is achieved.

INTRODUCTION

Photoinjector beam brightness has been increased by orders of magnitude, pushed by the development of ultrafast scientific instruments, such as hard X-ray FELs, Thomson scattering X-ray sources, ultrafast electron diffractometers and microscopes [1-4]. The electron beam brightness provided by state of the art photoinjectors is approaching the maximum beam brightness at cathode [5, 6]. The average beam brightness has also been pushed to the next level for development of high repetition rate ultrafast scientific instruments, such as ERL based X-ray source, MHz XFEL, and MHz ultrafast electron diffraction and microscopy [7-14]. Due to technical difficulty, current Continuous-Wave (CW) electron guns, such as DC, SRF and VHF gun, are limited to lower gradients and voltages than pulsed electron guns, and the beam transverse brightness is usually enhanced by moving the photoemission at cathode away from the ‘pancake’ regime into the ‘cigar’ regime, using a bunching cavity downstream the gun to compress the beam and inject into the booster linac [7, 15]. Unlike high gradient guns, CW electron injectors optimize the transverse brightness at the cathode, and recovers the peak current downstream the gun.

The number of optimization parameters in a CW electron injector is substantially increased by the complexity of the beamline, and relies heavily on multi-

objective genetic optimizer [16]. A genetic optimizer has been developed at LBNL for optimizing a MHz photoinjector based on a normal conducting VHF gun [15]. In the following, we use such a tool to revisit the optimization of an S-band photoinjector.

INJECTOR OPTIMIZATION BY USING GENETIC OPTIMIZER

A typical S-band injector, such as LCLS photoinjector, consists of a high gradient (~ 120 MV/m) S-band gun, an emittance compensation solenoid and two travelling wave linacs [1]. The beam brightness optimization usually is an iteration process. First the emittance compensation is performed by tuning the solenoid strength and first linac gradient; second, the laser transverse and longitudinal dimensions are tuned for achieving beam peak current, balancing between thermal emittance and space charge effects. The two processes are iterated until the minimum emittance is found. The whole optimization process is time consuming, and provides a single working point instead of a global picture of the trade-offs between beam emittance and bunch length.

The genetic optimizer is used to find global minima in a multi-objective optimization, and has been extensively used in CW photoinjector optimizations [8, 10]. An optimizer based on NSGA-II algorithm has been used at Berkeley to optimize both APEX and LCLS-II photoinjectors, and the beam dynamics are simulated with ASTRA code [17].

In the following, the same optimizer is used to investigate the dependence of the optimized S-band injector layout on bunch charge or peak current. Injector beam brightness is compared with the initial cathode beam brightness to give a sense of the beam quality preservation along the beamline. The BNL/LCLS type S-band injector with a gradient of 120 MV/m is used for case studies. The laser dimensions and the gun phase and solenoid strength are free parameters in the optimization. The voltages of the two travelling wave linacs are allowed to vary within 78 MV per linac, but phases are fixed to maximum acceleration. The entrance position of the first linac is allowed to vary to optimize injector layout. Beam energy at injector exit is constrained to be above 100 MeV, which is typical for most XFEL photoinjectors.

INJECTOR LAYOUT VS BUNCH CHARGE

The LCLS photoinjector was optimized for a 1 nC beam with 100 A peak current, but it is nowadays mostly working at lower charges, typically 250 pC [1, 18], with which it successfully achieved the first hard X-ray FEL lasing [19]. In this section, the bunch charge is varied

*This work was supported by the Director of the Office of Science of the US Department of Energy under Contract no. DEAC02-05CH11231 #hqian@lbl.gov

between 0 and 1 nC, and RMS bunch length is constrained to be shorter than 1 mm to include the original LCLS 1 nC solution. The laser transverse profile is a Gaussian distribution with one sigma radius truncation [20], and laser longitudinal distribution is a flat-top with rising and falling edge 10% of its FWHM duration. The thermal emittance of the cathode is set to be $0.9 \mu\text{m}/\text{mm}$ [21]. The purpose of this optimization is to investigate the optimized injector layout as a function of bunch charge or peak current.

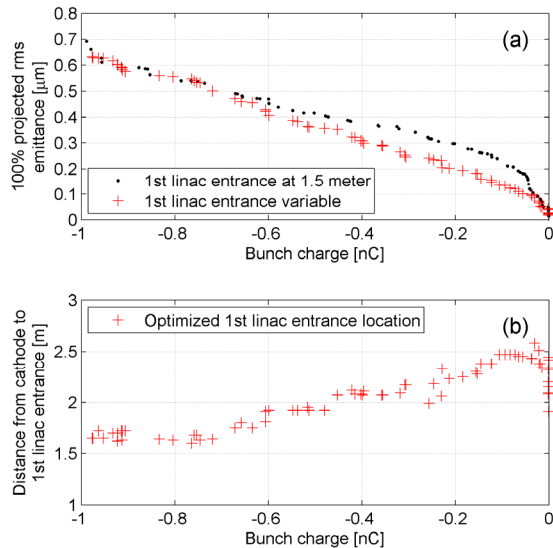


Figure 1: Injector layout optimizations (ASTRA simulations with 10 k macro particles), (a) Pareto front of emittance vs charge with RMS bunch length shorter than 1 mm and injector beam energy above 100 MeV, (b) optimized location of first linac entrance vs bunch charge.

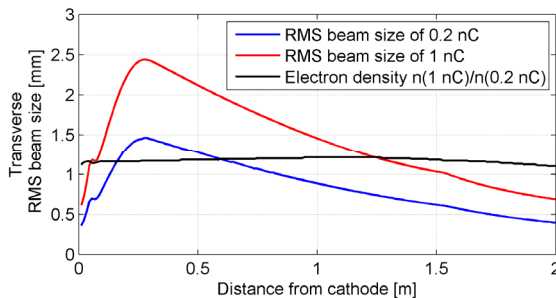


Figure 2: Transverse RMS beam size and electron density ratio between 1 nC & 0.2 nC when beam waist is focused at 1.5 meter, entrance of first booster linac.

The simulation results are shown in Fig. 1. The current LCLS injector layout is optimized for charges close to 1 nC. For lower charges, the optimized distance between cathode and first linac entrance tends to increase (Fig. 1(b)), getting to about 2.2 meters for 0.2 nC. The solutions of 1 nC and 0.2 nC are compared in Fig. 2, showing that, when both beams are focused at a distance of 1.5 m, the electron density of the 0.2 nC is lower, leading to a lower plasma frequency. Since the emittance compensation is one-half of a plasma period in the

transverse plane [22], it is clear that the 0.2 nC case should have a longer drift before injection into the first linac compared to 1 nC (Fig. 1(b)). Several photoinjectors optimized for 200 pC have already been designed with longer emittance oscillation drifts [23, 24].

TRADE-OFF BETWEEN EMITTANCE AND BUNCH LENGTH

Current hard X-ray FELs are operated at ~ 200 pC charge, where normalized emittance values down to 0.2–0.4 μm range have been obtained, depending on injector beam peak current [2, 3, 20]. Pushing such values to 0.1 μm would decrease the electron beam energy needed for reaching hard X-rays in X-FELs and substantially increase their performance [2, 25].

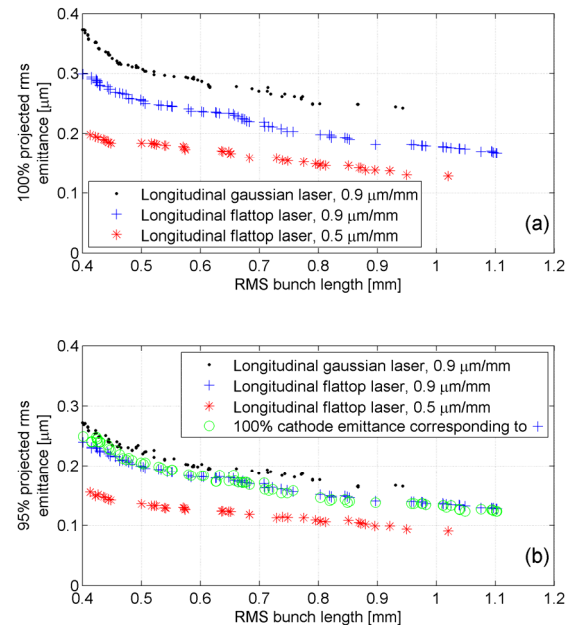


Figure 3: Pareto front of emittance vs rms bunch length for 200 pC bunch charge (ASTRA simulations with 10 k macro particles), (a) Pareto front of 100% emittance vs bunch length, (b) corresponding 95% emittance vs bunch length.

In the following we present a case study for 200 pC beam, showing the trade-off between emittance and bunch length. The impact of laser longitudinal distribution and thermal emittance on final beam emittance is also studied. The genetic optimizer was setup to minimize both the 100% emittance and RMS bunch length for 200 pC, and the tuning knobs and constraints are the same as those in the previous section.

The Pareto front of 100% emittance vs RMS bunch length for the 200 pC case is shown in Fig. 3, in which ~ 0.95 mm RMS bunch length corresponds to ~ 20 A peak current, and ~ 0.65 mm corresponds to ~ 30 A peak current. The 95% emittance is also displayed in Fig. 3(b) for reference, which is typically close to slice emittance. As seen from the Pareto front, emittance can be reduced as the beam peak current is lowered. Fig. 3(b) shows the

95% emittance of the beam is very close to the initial emittance at the cathode, meaning the beam core brightness is maintained over the transport, and is dominated by the initial cathode brightness.

Maximum cathode beam brightness is achieved close to photoemission saturation, i.e. when the accelerating RF electric field and space charge field on the cathode are of the same order. The saturation charge for ‘pancake’ and ‘cigar’ regime has been formulated as [5, 6]:

$$Q_{cigar}^{pancake} = eE_0 p R^2. \quad (1)$$

$$Q_{cigar} = \frac{\sqrt{2}}{9} I_0 \left(\frac{eE_0 R}{mc^2} \right)^2 t_{laser}^3. \quad (2)$$

where E_0 is the acceleration electric field during photoemission, R is laser radius, t_{laser} is laser duration, ϵ is vacuum permittivity, and $I_0 = 17$ kA is Alfven current. As pointed in Ref [6], when $R < t_{laser}^2 \cdot eE_0 / 2m_e$, photoemission is in the cigar regime.

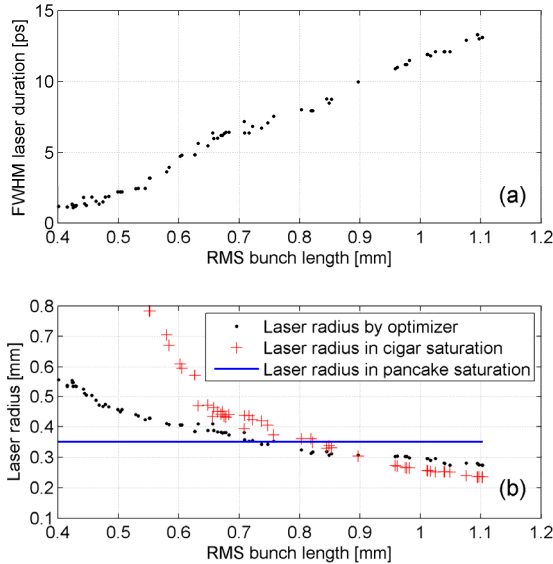


Figure 4: Laser radius and duration for 200 pC Pareto front solutions in Fig. 3 (longitudinal flat-top laser and 0.9 $\mu\text{m}/\text{mm}$), (a) Laser FWHM duration, (b) Laser radius.

Optimized laser duration and radius for the flat-top laser case are displayed versus the final RMS bunch length in Fig 4(a) and (b). In particular, Fig. 4(b) shows a comparison between the optimized laser radius from the Pareto front of Fig. 3 and the calculated laser radius in saturation for the ‘pancake’ and ‘cigar’ regime. In the ‘cigar’ regime, the photoemission is very close to max cathode brightness, while in the ‘pancake’ regime, the laser beam radius on the cathode increases very fast in order to achieve very short pulse lengths. Here the beam transverse brightness is not optimized anymore, since the optimizer is pushing charge emission away from saturation to avoid the pulse lengthening at the cathode.

The impact of laser longitudinal distribution on beam emittance is also compared. Fig.3 shows that 100% emittance of the longitudinal flat-top laser is clearly better than that of the Gaussian laser, but the advantage in 95% emittance is very small. Two solutions with 20 A peak current from the two different laser distributions are compared in Fig. 5, which shows the core slice emittance of the two laser distributions are almost the same, but the slice emittance of beam head and tail is much larger in the Gaussian laser case. In the pancake regime, the space charge of a beam produced by transversely truncated Gaussian laser was shown to be close to linear [20], and here simulations show such a laser distribution also works in the cigar regime to preserve the core beam brightness in S-band gun.

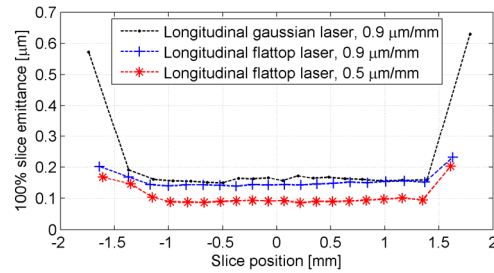


Figure 5: Slice emittance of 200 pC beam with 20 A peak current (ASTRA simulation with 200 k macro particles).

Since the injector beam core brightness is dominated by cathode beam brightness for the 200 pC case, reducing thermal emittance becomes critical to further increase injector beam brightness. As shown in Fig. 3 and 5, when thermal emittance is reduced to 0.5 $\mu\text{m}/\text{mm}$ [26-28], the slice emittance of 200 pC at 20 A can be reduced to 90 nm.

CONCLUSION

Genetic optimization of S-band photoinjector layout reveals a correlation between bunch charge, peak current and beamline length. As a case study, the trade-off between minimum achievable emittance and rms bunch length for a 200 pC beam was shown, and the dependence on longitudinal laser distribution and thermal emittance are discussed. Simulations show the max cathode beam brightness in the ‘cigar’ photoemission regime is preserved at injector exit for the 200 pC case. To increase beam peak current for the ‘cigar’ regime, a buncher cavity can be added downstream the gun [29]. It’s not practical to change drift distance after gun in an established photoinjector for optimizing different bunch charges, so ways to make photoinjector layout optimized for different charges will be investigated later.

ACKNOWLEDGMENT

The authors would like to thank Feng Zhou, Renkai Li, Zhirong Huang, Zhe Zhang for helpful discussions.

REFERENCES

- [1] R. Akre *et al.*, Phys. Rev. ST Accel. Beams 11, 030703 (2008).
- [2] E. Prat *et al.*, Phys. Rev. ST Accel. Beams 17, 104401 (2014).
- [3] M. Krasilnikov *et al.*, Phys. Rev. ST Accel. Beams 15, 100701 (2012).
- [4] R. Li *et al.*, Phys. Rev. Applied 2, 024003 (2014).
- [5] Ivan V. Bazarov *et al.*, Phys. Rev. Lett. 102, 104801 (2009).
- [6] D. Filippetto *et al.*, Phys. Rev. ST Accel. Beams 17, 024201 (2014).
- [7] Colwyn Gulliford *et al.*, Phys. Rev. ST Accel. Beams 16, 073401 (2013).
- [8] Colwyn Gulliford *et al.*, Appl. Phys. Lett. 106, 094101 (2015).
- [9] F. Sannibale *et al.*, Phys. Rev. ST Accel. Beams 15, 103501 (2012).
- [10] F. Sannibale *et al.*, in *Proc. of IPAC'16*, TUOCA02, these proceedings.
- [11] D. Filippetto *et al.*, J. Phys. B: At. Mol. Opt. Phys. 49, 104003 (2016).
- [12] S. Quan *et al.*, NIM A 798, 117 (2015).
- [13] A. Arnold *et al.*, Phys. Rev. ST Accel. Beams 14, 024801 (2011).
- [14] S. Belomestnykh, Proceedings of SRF'15, page 24.
- [15] C.F. Papadopoulos, Proceedings of IPAC'14, page 1974.
- [16] Ivan V. Bazarov *et al.*, Phys. Rev. ST Accel. Beams 8, 034202 (2005).
- [17] Klaus Floettmann, <http://www.desy.de/~mpyflo/>.
- [18] M. Ferrario *et al.*, SLAC-PUB-8400, 1999.
- [19] P. Emma *et al.*, Nature Photonics 4, 641 (2010).
- [20] F. Zhou *et al.*, Phys. Rev. ST Accel. Beams 15, 090701 (2012).
- [21] Y. Ding *et al.*, Phys. Rev. Lett. 102, 254801 (2009).
- [22] L. Serafini *et al.*, Phys. Rev. E 55, 7565 (1997).
- [23] S. Bettoni *et al.*, Phys. Rev. ST Accel. Beams 18, 123403 (2015).
- [24] J.-H. Han *et al.*, Proceedings of FEL'14, page 615.
- [25] B.E. Carlsten *et al.*, Proceedings of PAC'11, page 799.
- [26] H. Qian *et al.*, Appl. Phys. Lett. 97, 253504 (2010).
- [27] E. Prat *et al.*, Phys. Rev. ST Accel. Beams 18, 043401 (2015).
- [28] D.H. Dowell *et al.*, NIM A 622, 685 (2010).
- [29] Zhe. Zhang *et al.*, in *Proc. of IPAC'16*, WEPMY013, these proceedings.